JACS Au
AN OPEN ACCESS JOURNAL OF THE AMERICAN CHEMICAL SOCIETY

Open Access
This article is licensed under CC-BY 4.0

pubs.acs.org/jacsau
Letter

Identifying a Terminal Nickel−Oxygen Complex Bearing an Unsymmetrical β-Diketiminate Ligand

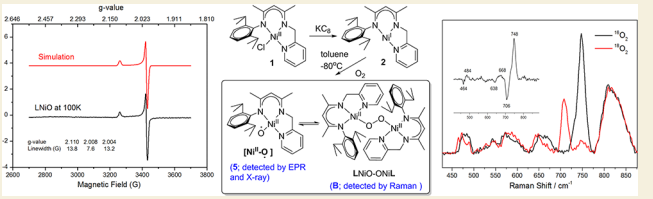
Si-Hong Chen, Tzu-Hsien Yang, Yu-Lun Chang, Wei-Syuan Lin, Chuan-Hung Chuang, Cheng-Han Yang, Hsing-Yin Chen,* Ming-Li Tsai,* and Sodio C. N. Hsu*

Cite This: https://doi.org/10.1021/jacsau.6c00356

Read Online

ACCESS | Metrics & More | Article Recommendations | Supporting Information

ABSTRACT: Nickel−oxygen species are proposed as key intermediates in various biological nickel-containing catalytic and enzymatic processes. We report the successful synthesis and crystallographic characterization of the first terminal nickel−oxygen complex featuring a tridentate *N*-aryl-*N*′-methylpyridyl β-diketiminate ligand. This species can be formally classified as either a nickel-oxo (Ni^{III}=O) or nickel-oxyl (Ni^{II}−$O^{\bullet}$) species, exhibiting dual bonding characteristics. The experimental observations and DFT calculations suggest the bonding is best described as a resonance hybrid of Ni^{III}=O and Ni^{II}−$O^{\bullet}$ states, with the Ni^{II}−$O^{\bullet}$ form likely predominant.



KEYWORDS: *β-Diketiminate, Terminal Ni−O, Chelation, Unsymmetrical, Nickel-oxyl, Hydrogen-atom abstraction*

Downloaded via KAOHSIUNG MEDICAL UNIV on May 11, 2026 at 02:44:32 (UTC).
See https://pubs.acs.org/sharingguidelines for options on how to legitimately share published articles.

Transition metal complexes featuring terminal oxo or oxyl ligation are proposed as key intermediates in numerous biological and abiological catalytic oxidation processes.[1−10] The isolation and synthesis of metal-oxo or -oxyl species could enhance our understanding of bioinspired chemistry. Nickel-oxo and nickel-oxyl species have attracted considerable attention because they have garnered significant interest due to their potential as intermediates in nickel-mediated oxidation reactions.[11−18] For example, a [Ni^{III}-oxo] species was proposed as the active oxidant in the $[Ni^{II}(TPA)]^{2+}$ [TPA = tris(2-pyridylmethyl)amine] catalyzed alkane hydroxylation.[14,15] Driess and co-workers suggested that a transient nickel−oxygen species [$L^{iPr}Ni$ = O ↔ $L^{iPr}Ni$−$O^{\bullet}$] (L^{iPr} = HC(CMeNC$_6H_3{}^{i}Pr_2$)$_2$) is generated through N_2O monooxygenation of [$(L^{iPr}Ni^{I})_2(\mu$-η^3:η^3-$C_6H_5Me)$], acting as a hydrogen scavenger and subsequently formed an unusual [$(L^{iPr}Ni^{II})_2(\mu$−OH)$_2$].[19] Additionally, experimental and theoretical studies propose a nickel−oxygen species as an effective oxidant for the challenging gas-phase conversion of methane to methanol.[20−22] Despite this, spectroscopic investigations of nickel−oxygen species remain limited, and no crystallographic characterization exists.[23−26]

Drawing inspiration from symmetrical β-diketiminato nickel(I) complexes[27−32] and prior studies on unsymmetrical β-diketiminato systems,[33−36] we propose that the *N*-aryl-*N*′-methylpyridyl β-diketiminate ligand (**L**H) acts as a hemilabile chelator. The flexible methylpyridyl arm provides electronic tunability and enables reversible coordination, allowing the ligand to adapt its denticity and stabilize high-valent or radicaloid nickel−oxygen units. This design creates an unsymmetric donor environment that promotes spin delocalization onto the oxygen atom, disfavors bimolecular decomposition, and facilitates reorganization from the T-shaped Ni(I) precursor (**2**) to a four-coordinate terminal Ni−O species (**5**). Accordingly, we report the crystallographic characterization of the first terminal nickel−oxygen complex supported by this tridentate ligand framework (Scheme 1).

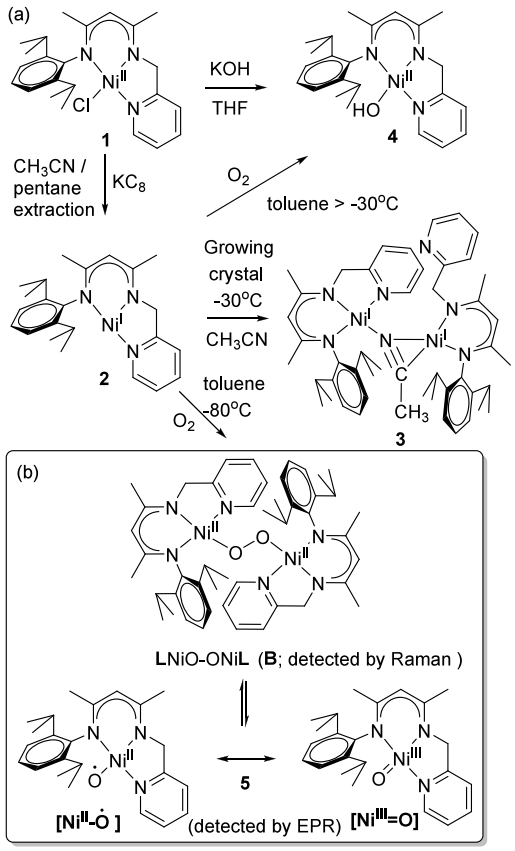
Deprotonation of LH with KO^{t}Bu in the presence of [$NiCl_2$(2,4-lutidine)$_2$] afforded **L**$Ni^{II}Cl$ (**1**), which was reduced with KC_8 to give the paramagnetic T-shaped Ni(I) complex **L**Ni^{I} (**2**). Both complexes have been independently reported,[37,38] our data are fully consistent with the literature. Complex **1** is diamagnetic and air-stable, while **2** is highly air- and moisture-sensitive, exhibiting a rhombic signal (g_1= 2.288, g_2 = 2.134, and g_3 = 2.035) with ^{14}N superhyperfine coupling (A_N = 17 G) to one ligand nitrogen and higher spin density on N2 (Figure 1, Table S3).[39−41]

Crystallization of **2** from pentane or hexane revealed the expected T-shaped geometry (Figure 2a). Interestingly, crystallization from acetonitrile gave an unexpected dinickel(I) species, **3**, where acetonitrile bridges two nickel centers in a μ-κ^1:η^2-bonding mode (Figure 2b). Notably, the N≡C bond length of 1.236(7) Å reflects back-bonding from the η^2-bound nickel(I) center, longer than the 1.157(9) Å in free acetonitrile.[42] The μ-κ^1:η^2-bound nitrile has been observed

Received: March 10, 2026
Revised: April 15, 2026
Accepted: May 5, 2026

© XXXX The Authors. Published by American Chemical Society

Scheme 1[a]



[a](a) Synthesis of the *N*-aryl-*N*′-methylpyridyl *β*-diketiminato nickel complexes. (b) Formation of **5** as a Ni^{III}=O or Ni^{II}−O$^{\bullet}$ species and its dinickel-peroxo species.

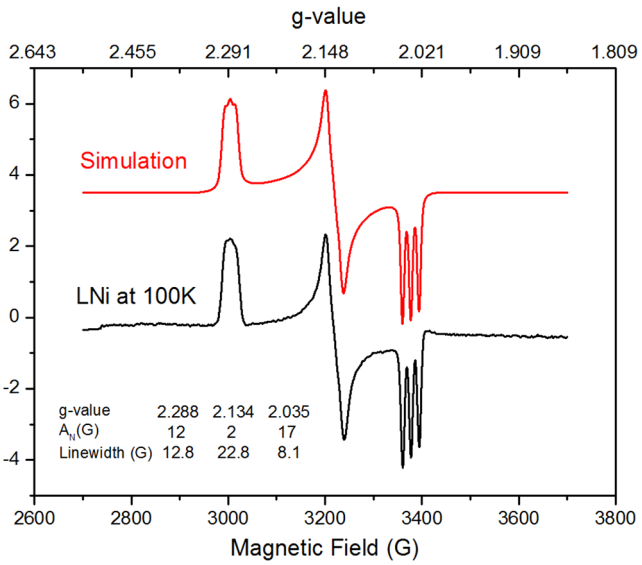


Figure 1. X-Band EPR spectra of **2** in toluene at 100 K.

with only selected transition metals[43] and has only been observed for nickel(0) species.[44,45]

Exposure of a toluene solution of **2** to dry dioxygen at ambient temperature triggered an immediate color shift from deep red to green, signaling the formation of the nickel(II)-hydroxyl species **L**Ni^{II}−OH (**4**). Fractional crystallization from

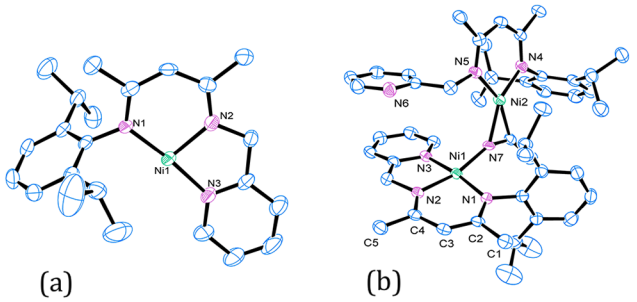


Figure 2. Molecular structure of (a) **2** and (b) **3**. Thermal ellipsoids are drawn at a 50% probability level. Hydrogen atoms are omitted for clarity.

the reaction mixture yielded green crystals of **4** in low yield (∼25%). The crystal structure, as shown in Figure S5, reveals a low-spin square-planar Ni(II) center with a terminal −OH group. The ^{1}H NMR spectra exhibit diagnostic peaks for the terminal hydroxyl (−4.73 ppm) and the *N*-aryl-*N*′-methylpyridyl *β*-diketiminate ligand framework (Figure S6). The Ni−O distance in **4** (1.854(2) Å) aligns with those of similar terminal nickel(II)-hydroxyl square-planar complexes.[46−49] The solid-state FTIR spectrum of isolated **L**Ni^{II}−OH (**4**) shows a distinct O−H stretch at ν(O−H) = 3637 cm^{-1}, shifted to ν(O−D) = 2633 cm^{-1} upon exposure to CH_3OD (Figure S7). Additionally, complex **4** can be prepared in a higher yield (82%) via salt metathesis from the reaction of **L**Ni^{II}Cl (**1**) with KOH.

A "side-on" superoxo-nickel complex, [L$^{i\mathrm{Pr}}$$Ni^{III}$(O$_2$)], with a symmetrical *β*-diketiminato ligand, was previously reported from the reaction of [(L$^{i\mathrm{Pr}}$$Ni^{I}$)$_2$($\mu$-$\eta^3$:$\eta^3$-$C_6H_5Me$)] with dry dioxygen at −78 °C.[19] This finding motivated us to reexamine the reaction of **2** with dry dioxygen at a lower temperature, in contrast to the room temperature reaction that produced **4**. Spectrophotometric titration of **2** with dioxygen at −80 °C showed a 2:1 Ni/O$_2$ ratio in spectral changes (Figures 3 and S8), suggesting the possible formation of a nickel-monooxygen species **5** or dinickel−peroxo species under these conditions.

To explore intermediates formed during the oxygenation of **2**, low-temperature Raman spectroscopy was performed by exposing a frozen solution of **2** to dioxygen at −80 °C. The resulting spectra exhibited three O$_2$ isotope-sensitive bands at 484, 668, and 748 cm^{-1}, which shifted to 464, 638, and 706 cm^{-1} with ^{18}O$_2$ substitution (Figure 4). These isotopic shifts, with ratios of ν(Ni−^{16}O)/ν(Ni−^{18}O) = 1.041 and ν-(^{16}O−^{16}O)/ν(^{18}O−^{18}O) = 1.060, are assigned to Ni−O and O−O stretching vibrations, respectively, aligning with previously reported nickel−oxygen species.[50,51] DFT calculations further support this assignment, identifying the 668 cm^{-1} band (theor. value 684 cm^{-1}) to Ni−O bond vibrations of **L**Ni−O$^{\bullet}$ (**5**). The 484 cm^{-1} (theor. value 523 cm^{-1}) and 748 cm^{-1} (theor. value 770 cm^{-1}) bands may attribute to the Ni−O and O−O vibrations, respectively, of a peroxo-bridged dinickel intermediate, **L**Ni−O−O−Ni**L** (**B**, see Figure S9).

To further probe the reaction pathway, UV−vis absorption spectra of **2** with dry dioxygen were monitored at 523 nm at 10-s intervals at −110 °C, revealing transient intermediate species during the conversion to **5** (Figure S10). Based on these data together with low-temperature Raman spectroscopy, we propose a three-step mechanism for the formation of **5** (Scheme S1): (i) initial binding of O$_2$ to **2** to form the Ni-η^1-superoxo species **L**Ni^{II}−O$_2^{\bullet-}$ (**A**); (ii) rapid dimerization of **A**

https://doi.org/10.1021/jacsau.6c00356
JACS Au XXXX, XXX, XXX−XXX

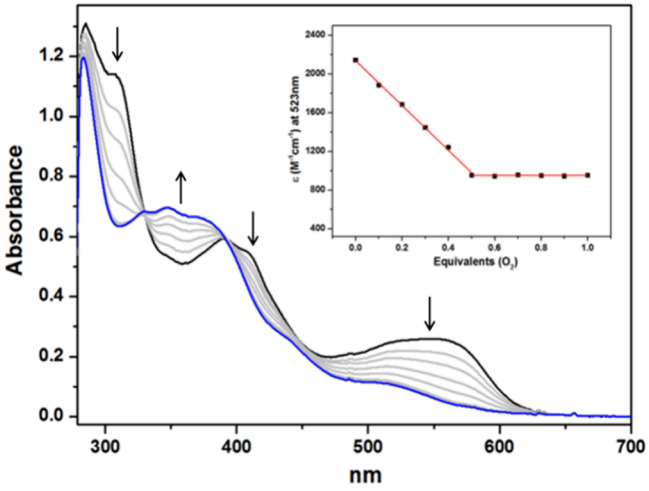


Figure 3. UV−vis changes accompanying oxygenation of **2** in toluene at −80 °C, using starting concentrations of 0.12 mM. The 0.1 equiv of oxygen was added at a rate of 2 per minute until 1.0 equiv was reached. The initial and final spectra are represented in black and blue, respectively. The insets show the results of spectrophotometric titrations of the complex **2** with O_2 at 523 nm, plotted as linear fits at a 2:1 Ni/O_2 ratio.

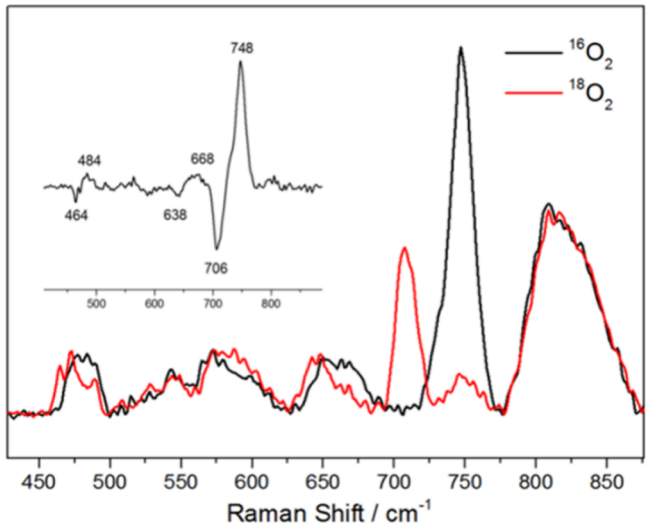


Figure 4. Raman spectra (λ_{ex} = 532 nm) of complex **2** recorded in MTHF at −80 °C prepared with $^{16}O_2$ (black) and partially $^{18}O_2$ labeled (red); inset: difference spectrum.

with a second equivalent of **2** to form the Ni_2-μ-1,2-peroxo species $LNi^{II}-O_2^{2-}-Ni^{II}L$ (**B**); and (iii) O−O bond homolysis of **B** to afford the nickel-monooxygen species **5** (Figure S9). DFT calculations indicate that the formation of **A** and **B** is thermodynamically favorable, and their binding modes are consistent with literature precedents.[51−53] The absence of superoxo vibrational features in the Raman spectra supports rapid conversion of **A** to **B**, underscoring the dynamic nature of the low-temperature oxygenation process.

A light-red crystal of **5** was obtained from the reaction mixture stored at −40 °C. The molecular structure of **5** reveals a square-planar nickel center bound by an oxygen atom and a tridentate *N*-aryl-*N*′-methylpyridyl β-diketiminate ligand (Figure 5). The Ni−O distance in **5** (1.750(4) Å) is shorter than the Ni−OH bond length in **4** (1.854(2) Å) and bis(μ-oxo)dinickel(III) complexes (~1.85(2) Å).[54−56] Additionally,

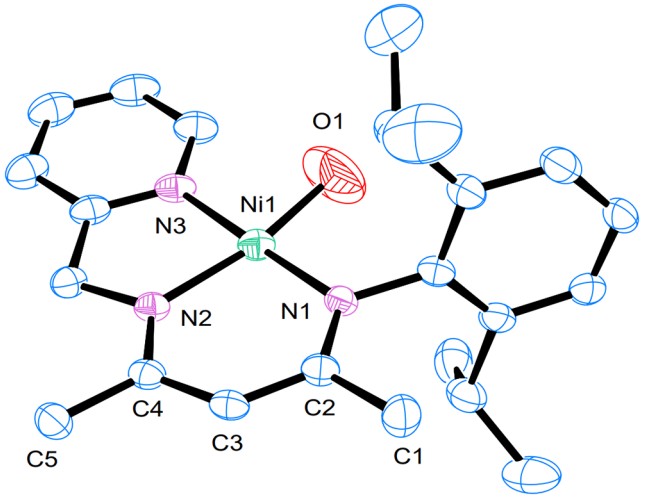


Figure 5. Molecular structure of **5**. Thermal ellipsoids are drawn at a 50% probability level. Hydrogen atoms are omitted for clarity.

it is shorter than the Ni−O distances in previously reported Ni^{II}_2(μ-1,2-peroxo)(1.834(2) Å)[51] and Ni^{III}_2(μ-1,2-peroxo)-(1.796(9) Å)[52] complexes. These comparisons indicate that **5** likely contains a terminal nickel(III)-oxo or nickel(II)-oxyl species.

Complex **5** is stable at −80 °C but decomposes rapidly above −30 °C. Monitoring the thermal decay by UV−vis spectra indicated a nickel(II)-hydroxyl species **4** formation, implying the hydrogen atom abstraction (HAA) reactivity of **5** (Figure S11). Variable-temperature EPR experiments confirmed this decay, with the characteristic signal of **5** diminishing above −30 °C (Figures S12−13). In-situ generation of **5** by bubbling O_2 into a toluene solution of **2** at −80 °C afforded an axial X-band EPR spectrum (g_1 = 2.110, g_2 = 2.008, g_3 = 2.004), well reproduced by simulation (Figure 6). Frontier molecular orbital analysis (Figure S17) reveals that the SOMO possesses significant d_{xz} character. Spin−orbit coupling with nearby filled d_{yz} (−4.72 eV) and d_{z^2} (−4.92 eV) orbitals accounts for the axial anisotropy and g-value deviation

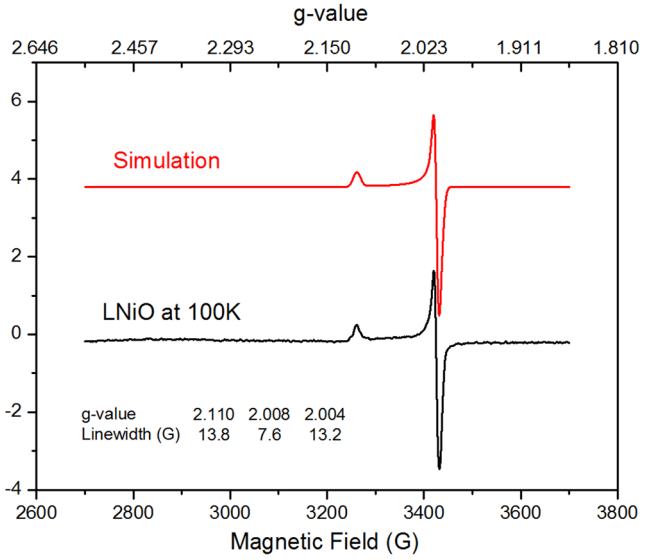


Figure 6. X-Band EPR spectra of *in situ* generated compound **5** in toluene at 100 K.

https://doi.org/10.1021/jacsau.6c00356
JACS Au XXXX, XXX, XXX−XXX

from g_e = 2.0023. These results indicate that the characteristic axial EPR signal arises from low-lying excited states and the specific d-orbital composition of the Ni-centered radical. EPR spin quantification of in situ oxygenated **2** samples revealed 41.8% conversion to the EPR-active nickel-monooxygen species **5** (Figure S14). Combined with the Raman data, this indicates a 1:0.7 equilibrium ratio between species **5** (41.8%) and the peroxo-bridged dinickel intermediate **B** (an EPR-silent μ-1,2-peroxo dinickel species; 29.1%) at −80 °C, suggesting that the 2 **L**Ni^{II}−O$^{\bullet}$ (or **L**Ni^{III}=O) ⇌ **L**NiO−ONi**L** equilibrium is slightly biased toward the oxyl pathway at −80 °C.

To investigate the mechanism of the oxidation pathway, N_2O was used as an alternative oxygen-atom source. UV−vis titration and in situ X-band EPR spectra confirmed formation of the same nickel-monooxygen species **5** observed with O_2 (Figure S15). Complementary resonance Raman measurements revealed the characteristic O−O stretching band at 748 cm^{-1} of the μ-1,2-peroxo dinickel intermediate **B** (**L**NiO−ONi**L**). The identical spectroscopic signatures obtained from both O_2 and N_2O indicate that the two oxidants converge on a common Ni−O intermediate. The simultaneous observation of **5** and **B** further supports a dynamic, reversible equilibrium between the terminal nickel−oxygen species and the peroxo-bridged dimer at low temperature.

To elucidate the bonding nature of the terminal nickel monooxygen species **5**, which can be formally classified as either **L**Ni^{III}=O or **L**Ni^{II}−O$^{\bullet}$, a molecular orbital (MO) analysis was conducted. As shown in Figure S17, MO93 corresponds to the σ-bonding interaction between the Ni $d_{x^2-y^2}$ and O p_x orbitals, with additional contributions from the ligand nitrogen atoms. MO104 and MO106 represent the two π-bonding interactions, while MO112 and the SOMO (MO113) are the corresponding π^* antibonding orbitals between Ni and O. Notably, the oxygen p_z orbital contributes substantially to the SOMO, indicating significant radical character on the terminal oxygen. As σ-bonding is stronger than π-bonding, MO93 lies lower in energy than the π-bonding MOs. Overall, six electrons occupy bonding orbitals (MO93, MO104, MO106) and three occupy antibonding orbitals (MO112 and SOMO113), affording a formal Ni−O bond order of 1.5. This was corroborated by natural population analysis (NPA), which indicated that the spin density is predominantly localized on the terminal oxygen (0.670 on O and 0.277 on Ni, Table S3). For more precise bond order data, Mayer, Wiberg, and Fuzzy bond order analyses were performed, and the values were 1.2, 1.6, and 1.8, respectively.[57] Therefore, the bonding nature of **5** can be best described as a resonance hybrid of Ni^{III}=O and Ni^{II}−O$^{\bullet}$ states, with the Ni^{II}−O$^{\bullet}$ form likely predominant.

To understand the chemical reactivity of **5**, stoichiometric reactions with PPh_3 and TEMPOH were performed. After treatment of **5** with PPh_3 at 183 K, followed by warming to room temperature, O=PPh_3 was obtained in 30% yield, as determined by ^{31}P NMR (Figure S18), indicating limited oxygen-atom transfer (OAT) reactivity. In contrast, the reaction of **5** with TEMPOH under identical conditions produced TEMPO radical and **L**Ni^{II}−OH (**4**) in 45% isolated yield after recrystallization. However, EPR spin quantification of the TEMPO radical revealed a significantly higher conversion of ca. 76% (Figures S19). No reactions occurred between **4** and TEMPO (Figure S21). These studies demonstrate that complex **5** exhibits efficient hydrogen atom abstraction (HAA) reactivity toward TEMPOH, while its OAT reactivity toward PPh_3 is comparatively limited. This dual reactivity profile is consistent with the resonance hybrid nature of the Ni^{III}=O and Ni^{II}−O$^{\bullet}$ states.

In summary, the *N*-aryl-*N*′-methylpyridyl β-diketiminate ligand framework stabilizes the nickel−oxygen unit, enabling the formation of a unique terminal nickel-monooxygen species **5** at low temperature. Based on the EPR data and DFT calculations, this paramagnetic nickel-monooxygen species **5** is best characterized as a resonance hybrid of Ni^{III}=O and Ni^{II}−O$^{\bullet}$ states with a planar tetracoordinate geometry. Additionally, low-temperature studies reveal a rapid equilibrium between the mononuclear oxyl **L**Ni−O$^{\bullet}$ and the peroxo-bridged dinickel intermediate **L**NiO−ONi**L**, highlighting the dynamic nature of the Ni−O system.

■ ASSOCIATED CONTENT

Supporting Information

The Supporting Information is available free of charge at https://pubs.acs.org/doi/10.1021/jacsau.6c00356.

Additional figures, tables, and crystallographic data (PDF)

Accession Codes

Deposition Numbers 2209936−2209939 and 2492714 contain the supplementary crystallographic data for this paper. These data can be obtained free of charge via the joint Cambridge Crystallographic Data Centre (CCDC) and Fachinformationszentrum Karlsruhe Access Structures service.

■ AUTHOR INFORMATION

Corresponding Authors

Hsing-Yin Chen − *Department of Medicinal and Applied Chemistry, Drug Development and Value Creation Research Center, College of Life Sciences, Kaohsiung Medical University, Kaohsiung 80708, Taiwan;* orcid.org/0000-0003-3948-8915; Email: hychen@kmu.edu.tw

Ming-Li Tsai − *Department of Chemistry, National Sun Yat-Sen University, Kaohsiung 80459, Taiwan;* orcid.org/0000-0003-2510-2866; Email: mltsai@mail.nsysu.edu.tw

Sodio C. N. Hsu − *Department of Medicinal and Applied Chemistry, Drug Development and Value Creation Research Center, College of Life Sciences, Kaohsiung Medical University, Kaohsiung 80708, Taiwan; Department of Chemistry, National Sun Yat-Sen University, Kaohsiung 80459, Taiwan;* orcid.org/0000-0002-2576-7289; Email: sodiohsu@kmu.edu.tw

Authors

Si-Hong Chen − *Department of Medicinal and Applied Chemistry, Drug Development and Value Creation Research Center, College of Life Sciences, Kaohsiung Medical University, Kaohsiung 80708, Taiwan;* orcid.org/0009-0009-4667-619X

Tzu-Hsien Yang − *Department of Medicinal and Applied Chemistry, Drug Development and Value Creation Research Center, College of Life Sciences, Kaohsiung Medical University, Kaohsiung 80708, Taiwan;* orcid.org/0000-0002-4360-8214

Yu-Lun Chang − *Department of Medicinal and Applied Chemistry, Drug Development and Value Creation Research Center, College of Life Sciences, Kaohsiung Medical*

https://doi.org/10.1021/jacsau.6c00356
JACS Au XXXX, XXX, XXX−XXX

University, Kaohsiung 80708, Taiwan; orcid.org/0000-0001-7085-5926

Wei-Syuan Lin − *Department of Medicinal and Applied Chemistry, Drug Development and Value Creation Research Center, College of Life Sciences, Kaohsiung Medical University, Kaohsiung 80708, Taiwan;* orcid.org/0000-0002-3191-1734

Chuan-Hung Chuang − *Department of Chemistry, National Sun Yat-Sen University, Kaohsiung 80459, Taiwan;* orcid.org/0009-0001-4492-0760

Cheng-Han Yang − *Department of Chemistry, National Sun Yat-Sen University, Kaohsiung 80459, Taiwan;* orcid.org/0009-0000-8958-1611

Complete contact information is available at: https://pubs.acs.org/10.1021/jacsau.6c00356

Notes

The authors declare no competing financial interest.

■ ACKNOWLEDGMENTS

This work was supported by the National Science and Technology Council of Taiwan, NSTC 111-2113-M-037-006, 111-2113-M-110-007, NSTC 113-2113-M-110-004. Additional support was provided by grants from the NSYSU-KMU Joint Research Project (NK111P13) and Kaohsiung Medical University (KMU-TB114009-2), Taiwan. The authors gratefully acknowledge the Joint Center for High Valued Instruments at National Sun Yat-Sen University and the Center for Research Resources and Development in Kaohsiung Medical University for the use of ESR, NMR, and crystallographic facilities.

■ REFERENCES

(1) Larson, V. A.; Battistella, B.; Ray, K.; Lehnert, N.; Nam, W. Iron and manganese oxo complexes, oxo wall and beyond. *Nat. Rev. Chem.* **2020**, *4* (8), 404−419.

(2) Shimoyama, Y.; Kojima, T. Metal-Oxyl Species and Their Possible Roles in Chemical Oxidations. *Inorg. Chem.* **2019**, *58* (15), 9517−9542.

(3) Elwell, C. E.; Gagnon, N. L.; Neisen, B. D.; Dhar, D.; Spaeth, A. D.; Yee, G. M.; Tolman, W. B. Copper-Oxygen Complexes Revisited: Structures, Spectroscopy, and Reactivity. *Chem. Rev.* **2017**, *117* (3), 2059−2107.

(4) Oloo, W. N.; Que, L. Bioinspired Nonheme Iron Catalysts for C-H and C = C Bond Oxidation: Insights into the Nature of the Metal-Based Oxidants. *Acc. Chem. Res.* **2015**, *48* (9), 2612−2621.

(5) Cook, S. A.; Borovik, A. S. Molecular Designs for Controlling the Local Environments around Metal Ions. *Acc. Chem. Res.* **2015**, *48* (8), 2407−2414.

(6) Nam, W. Synthetic Mononuclear Nonheme Iron-Oxygen Intermediates. *Acc. Chem. Res.* **2015**, *48* (8), 2415−2423.

(7) Puri, M.; Que, L. Toward the Synthesis of More Reactive S = 2 Non-Heme Oxoiron(IV) Complexes. *Acc. Chem. Res.* **2015**, *48* (8), 2443−2452.

(8) Gagnon, N.; Tolman, W. B. $[CuO]^{+}$ and $[CuOH]^{2+}$ Complexes: Intermediates in Oxidation Catalysis? *Acc. Chem. Res.* **2015**, *48* (7), 2126−2131.

(9) Nam, W.; Lee, Y.-M.; Fukuzumi, S. Tuning Reactivity and Mechanism in Oxidation Reactions by Mononuclear Nonheme Iron(IV)-Oxo Complexes. *Acc. Chem. Res.* **2014**, *47* (4), 1146−1154.

(10) Usharani, D.; Janardanan, D.; Li, C.; Shaik, S. A Theory for Bioinorganic Chemical Reactivity of Oxometal Complexes and Analogous Oxidants: The Exchange and Orbital-Selection Rules. *Acc. Chem. Res.* **2013**, *46* (2), 471−482.

(11) Corona, T.; Company, A. Spectroscopically Characterized Synthetic Mononuclear Nickel-Oxygen Species. *Chem.—Eur. J.* **2016**, *22* (38), 13422−13429.

(12) Yao, S.; Driess, M. Lessons from Isolable Nickel(I) Precursor Complexes for Small Molecule Activation. *Acc. Chem. Res.* **2012**, *45* (2), 276−287.

(13) Solans-Monfort, X.; Fierro, J. L. G.; Hermosilla, L.; Sieiro, C.; Sodupe, M.; Mas-Ballesté, R. O-O Bond activation in H_2O_2 and $(CH_3)_3C$-OOH mediated by $[Ni(cyclam)(CH_3CN)_2](ClO_4)_2$: Different mechanisms to form the same Ni(III) product? *Dalton Trans.* **2011**, *40* (26), 6868−6876.

(14) Nagataki, T.; Tachi, Y.; Itoh, S. Ni^{II}(TPA) as an efficient catalyst for alkane hydroxylation with m-CPBA. *Chem. Commun.* **2006**, No. 38, 4016−4018.

(15) Balamurugan, M.; Mayilmurugan, R.; Suresh, E.; Palaniandavar, M. Nickel(II) complexes of tripodal 4N ligands as catalysts for alkane oxidation using *m*-CPBA as oxidant: ligand stereoelectronic effects on catalysis. *Dalton Trans.* **2011**, *40* (37), 9413−9424.

(16) Pan, H.-R.; Wu, J.; Tsai, C.-M.; Liao, P.-J.; Hsu, H.-F. Basicity-Controlled C-H Bond Activation by a Structurally Characterized Ni(III)-Hydroxo Complex. *J. Am. Chem. Soc.* **2025**, *147* (31), 27855−27861.

(17) Mateos-Calbet, A.; Bruzzese, P. C.; Mermigki, M. A.; Schnegg, A.; Pantazis, D. A.; Cornella, J. Rapid Oxygen Atom Transfer at a Catalysis-Relevant Ni(I)-Alkyl Complex with N2O. *J. Am. Chem. Soc.* **2025**, *147* (23), 19438−19443.

(18) Lyakin, O. Y.; Talsi, E. P.; Bryliakov, K. P. Bioinspired Oxidations of C-H Groups Mediated by Nonheme Complexes of Late Transition Metals Co, Ni, and Cu. *ACS Catal.* **2025**, *15* (20), 17525−17547.

(19) Yao, S.; Bill, E.; Milsmann, C.; Wieghardt, K.; Driess, M. A "Side-on" Superoxonickel Complex $[LNi(O_2)]$ with a Square-Planar Tetracoordinate Nickel(II) Center and Its Conversion into $[LNi(\mu\text{-}OH)_2NiL]$. *Angew. Chem., Int. Ed.* **2008**, *47* (37), 7110−7113.

(20) Schröder, D.; Schwarz, H. C-H and C-C Bond Activation by Bare Transition-Metal Oxide Cations in the Gas Phase. *Angew. Chem., Int. Ed.* **1995**, *34* (18), 1973−1995.

(21) Pierpont, A. W.; Cundari, T. R. Computational Study of Methane C-H Activation by First-Row Late Transition Metal $L_nM{=}E$ (M: Fe, Co, Ni) Complexes. *Inorg. Chem.* **2010**, *49* (5), 2038−2046.

(22) Shiota, Y.; Yoshizawa, K. Methane-to-Methanol Conversion by First-Row Transition-Metal Oxide Ions: ScO^{+}, TiO^{+}, VO^{+}, CrO^{+}, MnO^{+}, FeO^{+}, CoO^{+}, NiO^{+}, and CuO^{+}. *J. Am. Chem. Soc.* **2000**, *122* (49), 12317−12326.

(23) Corona, T.; Pfaff, F. F.; Acuña-Parés, F.; Draksharapu, A.; Whiteoak, C. J.; Martin-Diaconescu, V.; Lloret-Fillol, J.; Browne, W. R.; Ray, K.; Company, A. Reactivity of a Nickel(II) Bis(amidate) Complex with meta-Chloroperbenzoic Acid: Formation of a Potent Oxidizing Species. *Chem.—Eur. J.* **2015**, *21* (42), 15029−15038.

(24) Pfaff, F. F.; Heims, F.; Kundu, S.; Mebs, S.; Ray, K. Spectroscopic capture and reactivity of S = 1/2 nickel(III)-oxygen intermediates in the reaction of a Ni^{II}-salt with *m*CPBA. *Chem. Commun.* **2012**, *48* (31), 3730−3732.

(25) Bok, K. H.; Lee, M. M.; You, G. R.; Ahn, H. M.; Ryu, K. Y.; Kim, S.-J.; Kim, Y.; Kim, C. Synthesis, Characterization, and Catalytic Activities of A Nickel(II) Monoamido-Tetradentate Complex: Evidence For Ni^{III}-Oxo and Ni^{IV}-Oxo Species. *Chem.—Eur. J.* **2017**, *23* (13), 3117−3125.

(26) Karmalkar, D. G.; Larson, V. A.; Malik, D. D.; Lee, Y.-M.; Seo, M. S.; Kim, J.; Vasiliauskas, D.; Shearer, J.; Lehnert, N.; Nam, W. Preparation and Characterization of a Formally NiIV-Oxo Complex with a Triplet Ground State and Application in Oxidation Reactions. *J. Am. Chem. Soc.* **2022**, *144* (49), 22698−22712.

(27) Pfirrmann, S.; Yao, S.; Ziemer, B.; Stösser, R.; Driess, M.; Limberg, C. β-Diketiminato Nickel(I) Complexes with Very Weak Ligation Allowing for H_2 and N_2 Activation. *Organometallics* **2009**, *28* (24), 6855−6860.

(28) Pfirrmann, S.; Limberg, C.; Herwig, C.; Stößer, R.; Ziemer, B. A Dinuclear Nickel(I) Dinitrogen Complex and its Reduction in Single-Electron Steps. *Angew. Chem., Int. Ed.* **2009**, *48* (18), 3357−3361.
(29) Kogut, E.; Wiencko, H. L.; Zhang, L.; Cordeau, D. E.; Warren, T. H. A Terminal Ni(III)-Imide with Diverse Reactivity Pathways. *J. Am. Chem. Soc.* **2005**, *127* (32), 11248−11249.
(30) Bai, G.; Wei, P.; Stephan, D. W. A β-Diketiminato-Nickel(II) Synthon for Nickel(I) Complexes. *Organometallics* **2005**, *24* (24), 5901−5908.
(31) Puiu, S. C.; Warren, T. H. Three-Coordinate β-Diketiminato Nickel Nitrosyl Complexes from Nickel(I)-Lutidine and Nickel(II)-Alkyl Precursors. *Organometallics* **2003**, *22* (20), 3974−3976.
(32) Holland, P. L.; Cundari, T. R.; Perez, L. L.; Eckert, N. A.; Lachicotte, R. J. Electronically Unsaturated Three-Coordinate Chloride and Methyl Complexes of Iron, Cobalt, and Nickel. *J. Am. Chem. Soc.* **2002**, *124* (48), 14416−14424.
(33) Chand, K.; Tsai, C.-L.; Chen, H.-Y.; Ching, W.-M.; Hsu, S.-P.; Carey, J. R.; Hsu, S. C. N. Improved Synthesis of Unsymmetrical N-Aryl-N′-alkylpyridyl ß-Diketimines Using Molecular Sieves and their Lithium Complexes. *Eur. J. Inorg. Chem.* **2018**, *2018* (9), 1093−1098.
(34) Chuang, W.-J.; Chen, H.-Y.; Chen, W.-T.; Chang, H.-Y.; Chiang, M. Y.; Chen, H.-Y.; Hsu, S. C. N. Steric and chelating ring concerns on the L-lactide polymerization by asymmetric β-diketiminato zinc complexes. *RSC Adv.* **2016**, *6* (43), 36705−36714.
(35) Chuang, W.-J.; Hsu, S.-P.; Chand, K.; Yu, F.-L.; Tsai, C.-L.; Tseng, Y.-H.; Lu, Y.-H.; Kuo, J.-Y.; Carey, J. R.; Chen, H.-Y.; Chen, H.-Y.; Chiang, M. Y.; Hsu, S. C. N. Reactivity Study of Unsymmetrical β-Diketiminato Copper(I) Complexes: Effect of the Chelating Ring. *Inorg. Chem.* **2017**, *56* (5), 2722−2735.
(36) Chand, K.; Chu, Y.-C.; Wang, T.-W.; Kao, C.-L.; Lin, Y.-F.; Tsai, M.-L.; Hsu, S. C. N. Nitric oxide generation study of unsymmetrical β-diketiminato copper(II) nitrite complexes. *Dalton Trans.* **2022**, *51* (9), 3485−3496.
(37) Pahar, S.; Sharma, V.; Mahata, B.; George, C. P.; Sharma, H.; Vanka, K.; Sen, S. S. Tridentate NacNac Stabilized Tin and Nickel Complexes: Access to a Monomeric Nickel Hydride and Its Catalytic Application. *Inorg. Chem.* **2022**, *61* (43), 17370−17377.
(38) Pahar, S.; Sharma, V.; Raj, K. V.; Sangole, M. P.; George, C. P.; Singh, K.; Vanka, K.; Gonnade, R. G.; Sen, S. S. Tridentate NacNac Tames T-Shaped Nickel(I) Radical. *Chem.—Eur. J.* **2024**, *30* (12), No. e202303957.
(39) Rettenmeier, C.; Wadepohl, H.; Gade, L. H. Stereoselective Hydrodehalogenation via a Radical-Based Mechanism Involving T-Shaped Chiral Nickel(I) Pincer Complexes. *Chem.—Eur. J.* **2014**, *20* (31), 9657−9665.
(40) Rettenmeier, C. A.; Wadepohl, H.; Gade, L. H. Electronic structure and reactivity of nickel(I) pincer complexes: their aerobic transformation to peroxo species and site selective C-H oxygenation. *Chem. Sci.* **2016**, *7* (6), 3533−3542.
(41) Griego, L.; Woods, T. J.; Mirica, L. M. A five-coordinate Ni(I) complex supported by 1,4,7-triisopropyl-1,4,7-triazacyclononane. *Chem. Commun.* **2022**, *58* (53), 7360−7363.
(42) Demaison, J.; Dubrulle, A.; Boucher, D.; Burie, J.; Typke, V. Microwave spectra, centrifugal distortion constants, and rz structure of acetonitrile and its isotopic species. *J. Mol. Spectrosc.* **1979**, *76* (1), 1−16.
(43) Michelin, R. A.; Mozzon, M.; Bertani, R. Reactions of transition metal-coordinated nitriles. *Coord. Chem. Rev.* **1996**, *147*, 299−338.
(44) Shoshani, M. M.; Beck, R.; Wang, X.; McLaughlin, M. J.; Johnson, S. A. Synthesis of Surface-Analogue Square-Planar Tetranuclear Nickel Hydride Clusters and Bonding to μ_4-NR, -O and -BH Ligands. *Inorg. Chem.* **2018**, *57* (5), 2438−2446.
(45) Stolley, R. M.; Duong, H. A.; Thomas, D. R.; Louie, J. The Discovery of $[Ni(NHC)RCN]_2$ Species and Their Role as Cycloaddition Catalysts for the Formation of Pyridines. *J. Am. Chem. Soc.* **2012**, *134* (36), 15154−15162.
(46) Huang, D.; Holm, R. H. Reactions of the Terminal Ni^{II}-OH Group in Substitution and Electrophilic Reactions with Carbon Dioxide and Other Substrates: Structural Definition of Binding Modes in an Intramolecular $Ni^{II}\cdots Fe^{II}$ Bridged Site. *J. Am. Chem. Soc.* **2010**, *132* (13), 4693−4701.
(47) Powell-Jia, D.; Ziller, J. W.; DiPasquale, A. G.; Rheingold, A. L.; Borovik, A. S. A structure and reactivity analysis of monomeric Ni(II)-hydroxo complexes prepared from water. *Dalton Trans.* **2009**, No. 16, 2986−2992.
(48) Adhikari, D.; Mossin, S.; Basuli, F.; Dible, B. R.; Chipara, M.; Fan, H.; Huffman, J. C.; Meyer, K.; Mindiola, D. J. A Dinuclear Ni(I) System Having a Diradical Ni_2N_2 Diamond Core Resting State: Synthetic, Structural, Spectroscopic Elucidation, and Reductive Bond Splitting Reactions. *Inorg. Chem.* **2008**, *47* (22), 10479−10490.
(49) Li, Y.; Fan, W.; Zhang, Z.; Xie, X.; Xiang, S.; Huang, D. Copper(II)-hydroxide facilitated C-C bond formation: the carboxamido pyridine system versus the methylimino pyridine system. *Dalton Trans.* **2020**, *49* (35), 12189−12196.
(50) Kieber-Emmons, M. T.; Schenker, R.; Yap, G. P. A.; Brunold, T. C.; Riordan, C. G. Spectroscopic Elucidation of a Peroxo Ni2(μ-O2) Intermediate Derived from a Nickel(I) Complex and Dioxygen. *Angew. Chem., Int. Ed.* **2004**, *43* (48), 6716−6718.
(51) Duan, P.-C.; Manz, D.-H.; Dechert, S.; Demeshko, S.; Meyer, F. Reductive O_2 Binding at a Dihydride Complex Leading to Redox Interconvertible μ-1,2-Peroxo and μ-1,2-Superoxo Dinickel(II) Intermediates. *J. Am. Chem. Soc.* **2018**, *140* (14), 4929−4939.
(52) Zhao, N.; Filatov, A. S.; Xie, J.; Hill, E. A.; Rogachev, A. Y.; Anderson, J. S. Generation and Reactivity of a Ni^{III2}(μ-1,2-peroxo) Complex. *J. Am. Chem. Soc.* **2020**, *142* (52), 21634−21639.
(53) McNeece, A. J.; Jesse, K. A.; Xie, J.; Filatov, A. S.; Anderson, J. S. Generation and Oxidative Reactivity of a Ni(II) Superoxo Complex via Ligand-Based Redox Non-Innocence. *J. Am. Chem. Soc.* **2020**, *142* (24), 10824−10832.
(54) Morimoto, Y.; Takagi, Y.; Saito, T.; Ohta, T.; Ogura, T.; Tohnai, N.; Nakano, M.; Itoh, S. A Bis(μ-oxido)dinickel(III) Complex with a Triplet Ground State. *Angew. Chem., Int. Ed.* **2018**, *57* (26), 7640−7643.
(55) Shiren, K.; Ogo, S.; Fujinami, S.; Hayashi, H.; Suzuki, M.; Uehara, A.; Watanabe, Y.; Moro-oka, Y. Synthesis, Structures, and Properties of Bis(μ-oxo)nickel(III) and Bis(μ-superoxo)nickel(II) Complexes: An Unusual Conversion of a $Ni^{III2}(\mu\text{-O})_2$ Core into a $Ni^{II2}(\mu\text{-OO})_2$ Core by H_2O_2 and Oxygenation of Ligand. *J. Am. Chem. Soc.* **2000**, *122* (2), 254−262.
(56) Hikichi, S.; Yoshizawa, M.; Sasakura, Y.; Komatsuzaki, H.; Moro-oka, Y.; Akita, M. Structural Characterization and Intramolecular Aliphatic C-H Oxidation Ability of $M^{III}(\mu\text{-O})_2M^{III}$ Complexes of Ni and Co with the Hydrotris(3,5-dialkyl-4-X-pyrazolyl)borate Ligands $Tp^{Me2,X}$ (X = Me, H, Br) and Tp^{iPr2}. *Chem.—Eur. J.* **2001**, *7* (23), 5011−5028.
(57) Lu, T.; Chen, F. Multiwfn: A multifunctional wavefunction analyzer. *J. Comput. Chem.* **2012**, *33* (5), 580−592.

https://doi.org/10.1021/jacsau.6c00356
JACS Au XXXX, XXX, XXX−XXX